International Journal of Power Electronics and Drive System (IJPEDS)
Vol. 17, No. 4, December 2026, pp. 2745~2756
ISSN: 2088-8694, DOI: 10.11591/ijpeds.v17.i4.pp2745-2756

Active clamp technique for voltage stress mitigation in flyback converters

Fauzan Ismail[1], Taufal Hidayat[1], Maaspaliza Azri[2], Yushaizad Yusof[3]
[1]Department of Electrical Engineering, Faculty of Engineering, Padang Institute of Technology, West Sumatra, Indonesia
[2]Department of Electrical Engineering, Universiti Teknikal Malaysia Melaka, Melaka, Malaysia
[3]Department of Electrical, Electronic & Systems Engineering, Faculty of Engineering & Built Environment, National University of Malaysia, Selangor, Malaysia

Article Info

Article history:

Received Dec 19, 2025
Revised Sep 9, 2026
Accepted Sep 13, 2026

Keywords:

Active clamp
Flyback converter
Leakage inductance
Switching loss
ZVS

ABSTRACT

Flyback converters are widely used in isolated low- to medium-power DC–DC conversion systems due to their simple structure, low component count, and inherent galvanic isolation. However, transformer leakage inductance causes severe drain-source voltage overshoot and high-frequency ringing during switch turn-off, leading to increased voltage stress, switching losses, electromagnetic interference, and reduced reliability. Passive RC snubbers are commonly used to suppress voltage spikes, but they dissipate leakage energy as heat, limiting converter efficiency, especially at higher switching frequencies. To address this limitation, this study experimentally investigates an active clamp flyback converter using a silicon carbide MOSFET (12M1H090) as the primary switching device. Three converter configurations are evaluated under comparable operating conditions: a conventional flyback converter, an RC-snubber-based flyback converter, and an active clamp flyback converter. The results show that the conventional flyback converter produces a peak drain-source voltage of approximately 380 V. At the same time, the active clamp configuration reduces the voltage stress to approximately 140 V. With optimized clamp capacitor, resonant inductance, and a 550 ns deadtime interval, zero-voltage switching is achieved, resulting in reduced switching stress. These findings demonstrate that coordinated tuning of active clamp parameters provides an effective approach for mitigating voltage stress and improving performance in high-frequency SiC-based flyback converters for microgrid, renewable energy, and auxiliary power supply applications.

This is an open access article under the CC BY-SA license.

Corresponding Author:

Fauzan Ismail
Department of Electrical Engineering, Faculty of Engineering, Padang Institute of Technology
St. Gajah Mada Kandis, Olo, Nanggalo, Padang, West Sumatra 25143, Indonesia
Email: fauzanismail@itp.ac.id

1. INTRODUCTION

The rapid growth of microgrids, renewable energy sources, and distributed energy resources has driven increased demand for small, high-efficiency, high-reliability, fully isolated DC–DC converters [1]–[3]. Within this category, the flyback converter topology is one of the most well-regarded for low- to medium-power applications due to its simple design, low component count, and inherent galvanic isolation. Consequently, flyback converters are a great fit for photovoltaic applications, battery storage system interfaces, electric vehicles, and industrial auxiliary power supply systems [4]–[7]. However, increasing power density and switching frequency pose greater challenges in the flyback converter, particularly in terms of efficiency, thermal management, and electromagnetic interference (EMI) [8]–[12]. Specifically, the concerns most

affecting the flyback converter are switching transitions and transformer leakage inductance; these two factors directly lead to increased overshoot, oscillations, and switching losses, all of which contribute to a lower economic standard of the converter within the specified appraisal range.

When the primary switch of a Flyback converter deactivates, the high-frequency switching generates a voltage spike across the switch. Therefore, if not adequately addressed, such spikes may surpass the switch's maximum rated drain-source voltage (V_{DS}), potentially resulting in switch failure. Furthermore, the presence of ringing and oscillations will lead to increased power dissipation in the converter and heightened EMI. The utilization of wide-bandgap (WBG) devices, such as silicon carbide (SiC), exacerbates the issue, regardless of the configuration [13]. This issue is attributable to the rapid switching of these devices, which entails swift transitions between on and off states, as well as elevated dv/dt that induces spikes to intolerable levels. Nevertheless, there is a trade-off with such WBG devices, for sure. They might have reduced energy losses, very low on-resistance, and withstand higher operational temperatures, but their fast-switching nature requires very careful design to adequately control the parasitic and snubber networks and avoid excessive stress from transients.

In high-efficiency power electronics, the deployment of fast-switching SiC MOSFETs introduces a complex multi-variable optimization challenge. At the hardware level, proper circuit design requires a simultaneous balance of device stress, conduction losses, gate-driver timing, parasitic capacitances, and thermal dissipation. Although SiC devices provide low on-state resistance, high breakdown voltage, and high-temperature capability, their rapid drain-source voltage transition can excite leakage-inductance resonance and parasitic-capacitance ringing if the clamp network and deadtime interval are not properly coordinated [14]. Therefore, the active clamp circuit in this work is evaluated not only as a voltage-spike mitigation method but also as a hardware-oriented solution to reduce switching stress and improve thermal reliability.

RC snubbers, or RCD clamps, are straightforward and proven methods to reduce voltage overshoot by trapping transient energy and damping oscillations. However, this method traps and dissipates leakage energy as heat, compromising its overall effectiveness and thermal performance, particularly at high switching frequencies or under changing load conditions [9], [10]. Therefore, in a bid to overcome the above problems and improve the overall efficiency of the converter, proposals based on active energy recovery techniques, such as the active clamp flyback (ACF) converter, which has attracted a lot of attention for recycling the unused leakage energy instead of dissipating it, have been put forward [15]–[17]. In this topology, the auxiliary switch and clamp capacitor (C_{clamp}) create a resonant path for limiting the voltage stress on the primary switch and allow a soft-switching mechanism (ZVS or ZCS) that further reduces switching losses and EMI [18]–[21].

Extensive research analyzed active clamp circuits and concluded that they are extremely useful, capable of achieving exceptional performance and efficiency when properly designed. For instance, it has been shown that by finely tuning clamp capacitance, leakage inductance, and deadtime between the main and auxiliary switches, one can achieve 96% efficiency and beyond, with claims spanning numerous studies [20], [22], [23]. Even so, sub-optimal soft-switching performance due to misalignment in the deadtime control, clamp capacitor (C_{clamp}), and resonant inductor (L_r) could result in improper energy recycling, circulating current, and voltage stress. In addition, active clamp designs based on WBG elements have received limited investigation. This phenomenon arises from the characteristics of several studies in the domain, which focus on simulation and low-power experiments [24]–[27]. Moreover, when using SiC devices, the nature of the circuitry with ultra-fast switching edges can, unfortunately but not uncommonly, result in large voltage overshot and amplified parasitic ringing if the timing is not optimized, along with the resonant parameters.

This research provides a detailed assessment of the performance of three distinct flyback converters, such as: i) a conventional flyback converter, ii) a flyback converter with RC snubber, and iii) an active clamp flyback converter configuration, focusing on voltage stress and oscillation behavior. The selected primary switching device is a SiC MOSFET chosen for its superior breakdown voltage and thermal performance. Furthermore, this work specifically addresses the limited experimental evidence on how SiC hardware behaviour and deadtime jointly influence voltage-stress mitigation. By demonstrating a 63% reduction in main switch voltage stress from 380 V to 140 V. This research provides a hardware-level analysis of SiC MOSFET operation in the active-clamp flyback converter. In addition, the findings are highly relevant to wider energy systems, where compact, isolated converters with reduced voltage stress are beneficial for battery charging interfaces and for distributed energy resources operating under variable load conditions.

The major contributions of this paper include the following:

i) Comparison of the active clamp flyback converter topology with RC-snubber and non-RC-snubber flyback topologies and analysis of their performance in the same test conditions.
ii) An experimental comparison of switching performance and thermal performance on switching devices with Si and SiC MOSFETs.
iii) An advanced active clamp configuration designed to achieve zero-voltage switching (ZVS) with a dead time of 550 ns, resulting in significantly reduced voltage stress and heightened ZVS efficiency.

iv) Migrating design insights to the coordinated selection of L_r, C_{clamp} and deadtime to further the switching performance and reliability of high-frequency WBG flyback converters.
v) A hardware-level interpretation of SiC MOSFET operation in the active clamp flyback converter, including device stress, conduction loss, parasitic-capacitance effects, gate-driver constraints, thermal implications, drive-system relevance, energy-system applicability, and benchmarking against other flyback stress-mitigation techniques.

The subsequent portions of this work are structured as follows: i) Section 2 examines the theory and design of the flyback converter, RC snubber, and active clamp circuit; ii) Section 3 examines the experimental setup and outcomes and discusses the results; and iii) Section 4 concludes the research by summarizing key points and offering design recommendations to improve the performance of flyback converters using SiC technology.

2. FLYBACK CONVERTERS

As shown in Figure 1(a), the flyback converter is an isolated DC-DC converter that stores energy in the magnetizing inductance of the coupled transformers during the switch-on time and then releases it to the secondary side during the switch-off time. In contrast to forward converters, the flyback transformer operates as a coupled inductor, serving as a genuine energy-transfer apparatus, with energy storage and delivery occurring sequentially during each switching cycle. During the ON state, the primary switch (S_{main}), is turned on and the input voltage (V_{in}) is turned on across the primary coil (N_p), causing the switching magnetization current (i_m) to increase linearly by as shown in (1).

$$i_m(t) = \frac{V_{in}}{L_m} t \tag{1}$$

Where L_m is the transformer magnetizing inductance. During this time, the secondary diode (D_o) is reverse-biased and isolating the output. When S_{main} goes OFF, the energy stored in L_m is sent to the secondary through a transformer. The secondary diode is now forward-biased, and the energy stored in the core is being delivered to the load. The output voltage is equal to the turns ratio times the voltage that comes back to the primary as expressed in (2).

$$V_O = \frac{N_s}{N_p}\left(V_{in} - V_{DS,off}\right) \tag{2}$$

Where N_s/N_p is the transformer turns ratio and V_{DS_off} is the voltage across the main switch during the OFF state.

The voltage spike across the switch when it is turned off is a major problem with the standard flyback converter. It happens because of leakage inductance (L_{Lk}) in the transformer. When S_{main} turns OFF abruptly, the energy stored in L_{Lk} cannot be transferred to the secondary winding, resulting in a transient overvoltage across the switch. This can be expressed as in (3).

$$V_{DS,peak} = V_{in} + \frac{N_p}{N_s} V_O + V_{Lk} \tag{3}$$

V_{Lk} is the voltage produced during the discharge of the leakage inductance, which is crucial to manage. Otherwise, the voltage can become so high that it exceeds the switch's voltage rating, causing switch breakdown and/or increased EMI from the hardware. To manage leakage-voltage overshoot, energy management networks such as RC snubbers and active clamp circuits are used to either dissipate or recycle the leakage energy.

In case of RC snubber implementation for flyback converter, a simple passive damping network consisting of a resistor (R_s) and a capacitor (C_s) arranged in parallel with the switch as in Figure 1(b). During the switch turn-off transient, C_s absorbs the leakage energy, temporarily decreasing the rate of voltage rise (dv/dt). Thereafter, the energy in C_s is lost as heat through R_s, according to (4).

$$E_{snub} = \frac{1}{2} C_s\left(V_{DS,peak}^2 - V_{DS,nom}^2\right) \tag{4}$$

Although it can limit voltage stress and reduce ringing, the RC snubber is a dissipative solution that negatively impacts overall converter efficiency. This efficiency drop is prominent at higher switching frequencies. The dissipated energy in R_s adds thermal stress, making this technique less favourable for high-density microgrid converters.

The ACF converter improves on passive techniques by not dissipating leakage energy. In ACF, an auxiliary switch (S_{clamp}) and clamp capacitor (C_{clamp}) are added in series, establishing a resonant network

with the transformer leakage inductance (L_{Lk}) as shown in Figure 1(c). When S_{main} turns off, the energy stored in L_{Lk} is resonantly transferred to C_{clamp} through S_{clamp}. This controlled energy transfer suppresses the voltage spike and charges of C_{clamp} to a predictable clamp voltage (V_{clamp}) as given in (5).

$$V_{clamp} = \frac{L_{Lk}}{C_{clamp}}\left(\frac{di}{dt}\right) \quad (5)$$

In the subsequent switching cycle, part of the energy stored in C_{clamp} is returned to the input through S_{main} to perform energy recovery and soft-switching operation. By appropriately adjusting the resonant parameters (L_{Lk}, C_{clamp}) and the deadtime td between S_{main} and S_{clamp}. The converter can achieve ZVS for both switches. As a result, switching losses and EMI are minimized, thereby improving the overall efficiency compared to conventional designs.

Also, with respect to the timing coordination between the main and clamp switches, the performance of the active clamp topology depends directly on it. A deadtime interval is implemented to avoid simultaneous conduction and to allow proper resonant energy transfer. First, if the deadtime is excessively short, both switches can produce shoot-through current if they overlap. Second, if it is too long, the resonant transition is incomplete, preventing ZVS and reintroducing voltage stress. The ideal deadtime ($t_{d,opt}$) satisfies the condition in (6).

$$t_{d,opt} \approx \frac{\pi}{2}\sqrt{L_{Lk}C_{clamp}} \quad (6)$$

During the deadtime interval, the active clamp flyback converter operates in a resonant mode formed by the resonant inductance L_r, and the parasitic output capacitance C_{oss} of the MOSFET), and the equivalent capacitance $C_{eq} = C_{oss} + C_{clamp}$. The natural resonant frequency is given by $\omega_r = 1/\sqrt{L_r C_{eq}}$. The drain-source voltage evolves with LC resonance, enabling energy exchange between the inductive and capacitive elements. Zero-voltage switching is achieved when the deadtime t_d is sufficiently long for the resonant transition to discharge the MOSFET output capacitance such that $v_{DS}(t_d) = 0$. This condition leads to a design constraint $t_d \geq \frac{\pi}{2}\sqrt{L_r C_{eq}}$, showing that ZVS operation is strongly dependent on the coordinated selection of L_r, C_{clamp}, and deadtime.

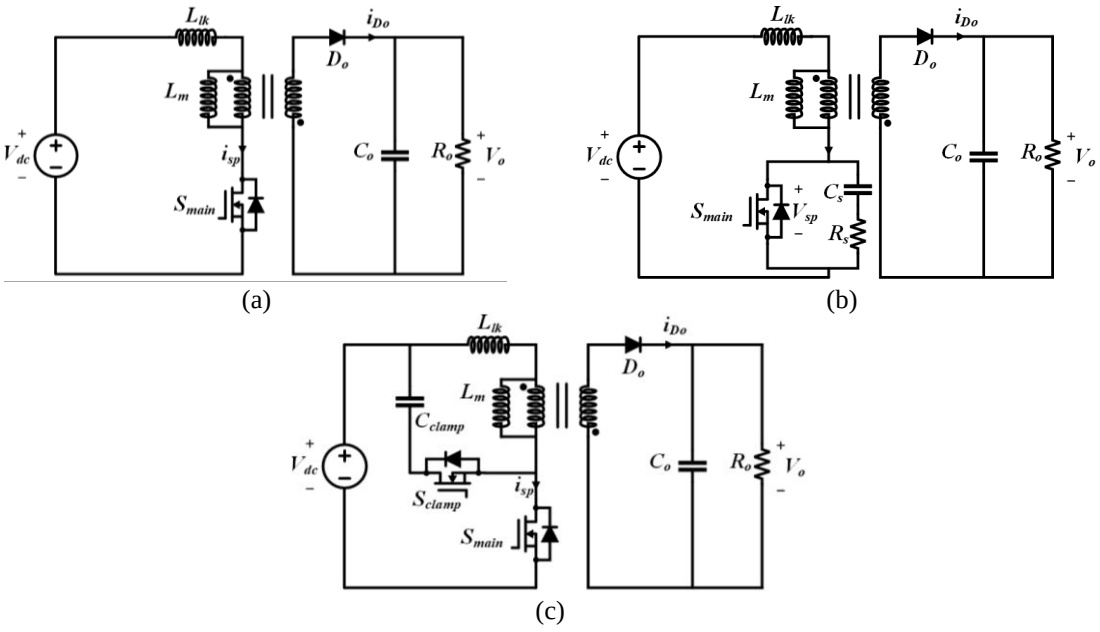

Figure 1. Flyback converter: (a) without RC snubber, (b) with RC snubber, and (c) with active clamp circuit

For clarity, the analytical presentation is focused on the three ZVS-governing parameters: the resonant inductance L_r, the clamp capacitance C_{clamp}, and the dead-time interval t_d. L_r and C_{clamp} determine the resonant transition rate, while t_d provides the required time interval for the drain-source voltage of the main

MOSFET to discharge before gate activation. If t_d is shorter than the resonant transition time, ZVS cannot be fully achieved; if t_d is excessively long, additional circulating loss and incomplete energy recovery may occur. Therefore, the design objective is not only to minimize the voltage spike, but also to coordinate L_r, C_{clamp}, and t_d so that the MOSFET turns on near the minimum VDS point.

3. RESULTS AND DISCUSSION

Figure 2 shows the experimental prototype of the flyback converter. To validate the proposed design and assess switching performance improvements, an experimental prototype of three flyback converter configurations was developed and tested under identical operating conditions. The configurations include: i) a conventional flyback converter, ii) a flyback converter with an RC snubber network, and iii) an ACF topology. The experiment has been configured based on the parameters listed in Table 1.



Figure 2. Prototype active clamp flyback converter

Table 1. Proposed system parameters

Parameter	Symbol	Value/device
Input voltage	V_{in}	30-36 V
Output voltage	V_O	280-400 V
Output power	P_O	100 W
Switching frequency	f_s	50 kHz
Transformer turns ratio	N_p/N_s	1:12
Magnetizing inductance	L_m	28 µH
Leakage inductance	L_{Lk}	1.73 nH
Main switch	S_m	SiC MOSFET 12M1H090
Clamp capacitor	C_{clamp}	50 nF
R snubber	R_s	22 Ω
C snubber	C_s	1 nF
Deadtime interval	t_{db}	550 ns

3.1. Traditional flyback converter

Figure 3 presents the experimental switching waveforms of the traditional flyback converter using the SiC MOSFET 12M1H090. The yellow trace denotes the gate-to-source voltage (V_{GS}), the purple trace represents the drain-to-source voltage (V_{DS}), and the green trace shows the output voltage (V_{OUT}). The converter operated at approximately 20 kHz under a 30 V input and nominal load condition. A pronounced voltage overshoot was observed at the moment of switch turn-off, with V_{DS} peaking between 375 V and 380 V. This transient spike originates from the transformer leakage inductance, which retains residual energy when the primary current is suddenly interrupted. In the absence of a snubber or an energy-recovery network, this energy excites a high-frequency resonant oscillation between the leakage inductance and the device's output capacitance. The oscillation frequency, observed in the megahertz range, induces significant ringing on V_{DS}, increasing device voltage stress and EMI. Although the SiC MOSFET exhibits fast switching transitions, low

on-resistance, and minimal turn-off energy, its high dv/dt and low parasitic capacitance amplify the overshoot phenomenon. Consequently, the conventional flyback configuration demonstrates poor transient damping and substantial switching stress, which may compromise reliability during high-temperature or dynamic-load operation. These results clearly highlight the need for snubbers or active clamps to limit voltage spikes and improve switching performance in SiC-based converters.

3.2. Flyback converter with RC snubber

Figure 4 shows the measured switching waveforms of the flyback converter equipped with an RC snubber network (R = 5 Ω, C = 100 nF) connected across the primary switch. The yellow trace represents the gate-to-source voltage (V_{GS}), the purple trace indicates the drain-to-source voltage (V_{DS}), and the green trace shows the output voltage (V_{OUT}). The converter operated at approximately 20 kHz to evaluate the snubber's damping performance at low-frequency switching conditions. The inclusion of the RC snubber effectively reduced the peak drain-source voltage from approximately 380 V to 320 V, confirming successful suppression of transient overshoot. The snubber capacitor (C_s) absorbs the leakage energy released at the moment of switch turn-off, while the resistor (R_s) dissipates this energy gradually as heat. As a result, the high-frequency ringing observed in the traditional configuration was substantially attenuated, resulting in a smoother, more stable turn-off transition. Although the RC snubber introduces a minor efficiency penalty due to resistive power dissipation, it markedly improves switching stability, mitigates EMI, and reduces device voltage stress, thereby enhancing converter reliability. However, since the leakage energy is dissipated rather than recycled, the RC snubber remains an energy-loss-based solution, and further improvement can be achieved through regenerative methods such as active clamp circuits that recover this energy and enable soft-switching operation.

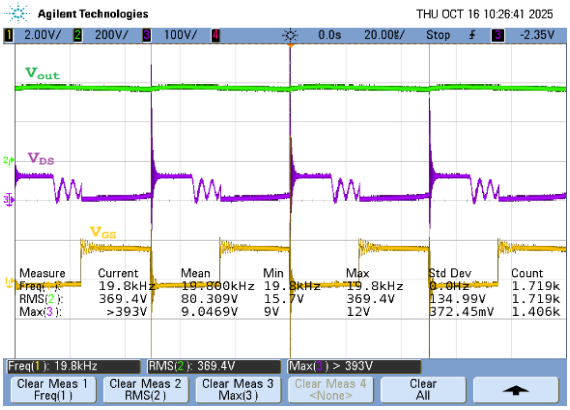

Figure 3. Traditional flyback converter

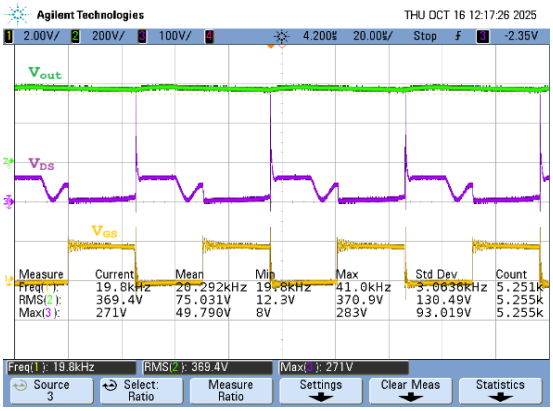

Figure 4. Flyback converter with RC-snubber

3.3. Active clamp flyback (ACF) converter

The experimental validation of the ACF Converter, utilizing a 12M1H090 SiC-MOSFET and an active clamp topology, is presented in Figure 5. The active clamp circuit comprises a clamp switch, a clamp capacitor (C_{clamp}) and a resonant inductor (L_r). These components play a crucial role in regulating voltage stress and energy efficiency, particularly in reducing voltage spikes and oscillations during operation. The primary objective of the experiment was to evaluate the impact of C_{clamp} and L_r on voltage spike behavior and oscillation reduction. The experimental results illustrate the effect of varying C_{clamp} values, alongside the implementation of L_r, on the voltage stress experienced by the switching components in the converter circuit.

As depicted in Figure 5(a), the circuit with a 20 µF C_{clamp}, without the inclusion of L_r, resulted in a noticeable ripple in the output voltage (V_O) and a high voltage spike of 380 V on the main switch (V_{DS_main}). This behavior suggests that the absence of L_r allows for greater voltage stress on the switching components, potentially reducing the system's longevity and reliability. The oscillation on the clamp voltage (V_{DS_clamp}) also contributes to instability in the converter operation, increasing the likelihood of failure in high-stress conditions. To address this, Figure 5(b) illustrates the implementation of L_r = 26 µH in the active clamp circuit. The addition of L_r mitigates the ripple in V_{DS_clamp}, effectively reducing the unwanted oscillations in the clamp circuit. However, this improvement comes at the cost of an increased spike in the V_{DS_clamp} waveform. This trade-off indicates that while L_r aids in stabilizing the converter's behavior and reducing ripple, but it does not entirely eliminate the risk of high-voltage spikes, which can still affect the overall performance and efficiency of the ACF converter.

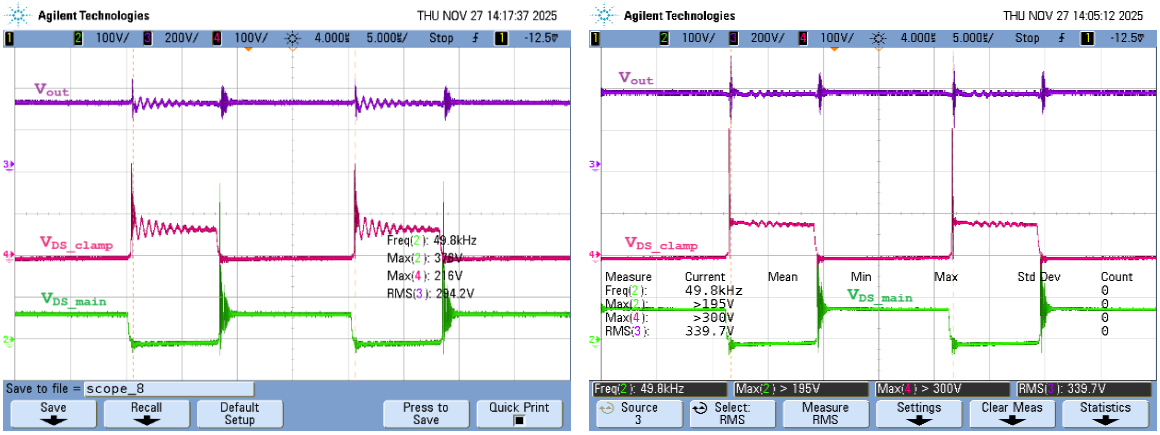

Figure 5. ACF circuit test: (a) C_{clamp} = 20 uF, L_r = 0; and (b) C_{clamp} = 20 uF, L_r = 26 uH

In this set of experiments, the values of the clamp capacitor (C_{clamp}) and resonant inductor (L_r) to reduce voltage spikes and oscillations in the ACF Converter circuit is optimized. The primary goal was to balance the values of C_{clamp} and L_r to minimize the ripple and stress on both the clamp voltage (V_{DS_clamp}) and the main switch voltage (V_{DS_main}), thereby improving the converter's efficiency and reliability. As shown in Figure 6(a), the circuit was tested with a 50 nF C_{clamp} and L_r = 0. The results revealed a 45 V oscillation on V_{DS_clamp}, with V_{DS_main} exhibiting spikes reaching 150 V. While the oscillations on V_{DS_main} were reduced compared to previous tests, the presence of significant spikes indicated that higher C_{clamp} values can still cause voltage stress on the main switch, highlighting the need for a more balanced approach between C_{clamp} and L_r to further minimize voltage spikes. To address this, Figure 6(b) illustrates the experiment with C_{clamp} set to 50 nF and L_r = 1.73 nH. With the addition of L_r, the V_{DS_clamp} oscillation was reduced to 25 V, with minimal ripple, and the V_{DS_main} spikes decreased to 140 V, accompanied by less oscillation. These results validate that the introduction of L_r helps in reducing both the spike and oscillation on V_{DS_clamp} and V_{DS_main}, demonstrating the effectiveness of the active clamp circuit in stabilizing the converter's operation and reducing voltage stress on the main switching components.

Figure 7 presents the key experimental waveforms of the proposed active-clamp flyback converter operating under soft-switching conditions. The resonant current flowing through the clamp network, I_{LR}, exhibits a sinusoidal profile during the transition interval, confirming the expected resonance between the leakage inductance and the clamp capacitor. This resonant action shapes both the main switch drain–source voltage V_{DS_main} and the clamp-node voltage V_{DS_clamp}, which transition smoothly rather than abruptly. The absence of sharp voltage edges indicates that the clamp circuit effectively absorbs and recycles the leakage energy, while the output waveform V_O aligns with the secondary conduction interval of the flyback stage, verifying proper power transfer operation.

A crucial observation in Figure 7 is that the main MOSFET turns on when its drain–source voltage has already been reduced to a low level via resonant discharge, demonstrating ZVS. The circulating current in I_{LR} provides the necessary energy to discharge the device's output capacitance before full gate activation, thereby minimizing switching losses and reducing voltage stress across the switch. The resonant transition of both V_{DS_main} and V_{DS_clamp} confirms that the converter is successfully operating in soft-switching mode. Overall, the measured waveforms validate that the active-clamp technique enables efficient energy recovery, lowers EMI, and enhances the overall performance of the flyback converter.

In addition to the observed reduction in voltage stress and soft-switching behavior, the measured waveforms also provide a qualitative indicator of better device performance. Switching energy, conduction loss, and gate-driver effects were not directly evaluated in this experiment, but their influence may be inferred from the SiC MOSFET properties and the waveform behavior shown in Figure 7. The lower peak V_{DS_main} and the more gradual voltage shifts during active-clamp operation imply less switching stress, principally due to less voltage-current overlap resulting from resonant energy transfer. Furthermore, the low $R_{DS}(on)$ characteristics of the SiC MOSFET contribute to a reduction in conduction loss, and the use of controlled deadtime and gentle transitions aids in the reduction of high (dv⁄dt) related gate difficulties such as the Miller effect and false turn-on. The results thus support a qualitative interpretation that the active clamp operation improves switching behaviour, reduces device stress, and enhances the overall reliability of the flyback converter.

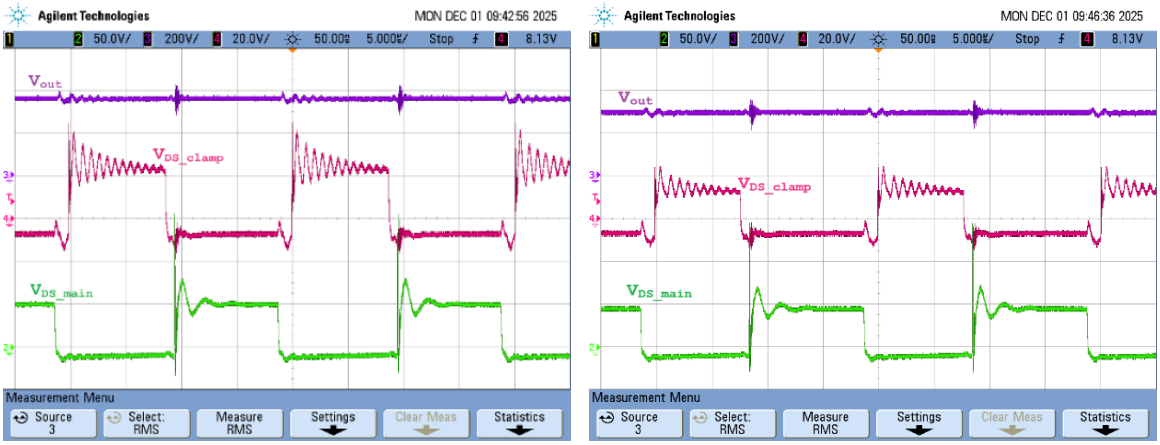

(a) (b)

Figure 6. ACF circuit test: (a) C_{clamp} = 50 nF, L_r = 0, and (b) C_{clamp} = 50 nF, L_r = 1.73 nH

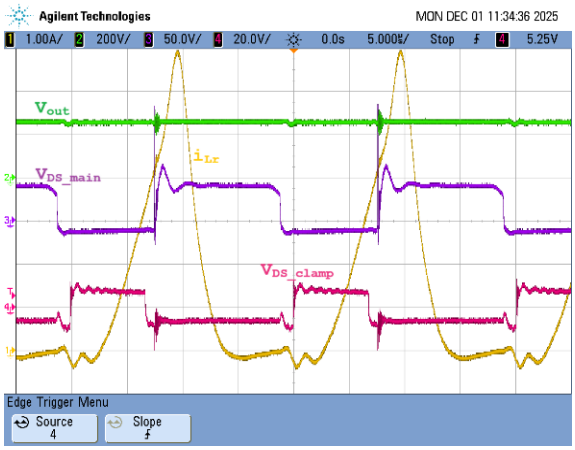

Figure 7. Soft-switching implementation on ACF circuit

3.4. SiC MOSFET switching dynamics, parasitic effects, and thermal interpretation

A deeper physical interpretation of the switching behavior can be established by considering the intrinsic characteristics of the SiC MOSFET used in this study. The device exhibits low output capacitance (C_{oss}) and gate-drain capacitance (C_{GD}), which strongly influence high-frequency switching transients. During switching events, the interaction between these parasitic capacitances and the transformer leakage inductance governs voltage overshoot, resonant oscillation, and the overall switching trajectory observed in the experimental waveforms. In the proposed active clamp operation, the leakage energy that would otherwise increase switching stress is redirected to the clamp capacitor via a resonant energy-exchange mechanism. This reshapes the switching transition into a controlled resonant waveform, reducing voltage–current overlap and switching stress, consistent with the reduced peak drain-source voltage observed in Figure 7.

Although switching energy and gate signals are not directly measured, the waveform behavior provides clear qualitative evidence of improved switching dynamics. The reduced voltage overshoot indicates lower turn-off stress, while the near-zero voltage condition before turn-on confirms partial or full ZVS operation, resulting in reduced switching losses. From a gate driver perspective, SiC MOSFETs are sensitive to parasitic inductances and Miller capacitance effects under high dv/dt conditions; however, the implemented deadtime and resonant commutation mitigate these effects by softening switching transitions. Thermally, reduced switching stress implies lower switching energy dissipation per cycle, thereby reducing junction temperature rise and improving device reliability under high-frequency operation. Overall, the interaction between parasitic capacitances, leakage inductance, and active clamp resonance provides a complete qualitative explanation of the improved switching performance of the proposed converter.

3.5. Discussion

Table 2 presents a comparative summary of the experimental results for three flyback converter configurations: the traditional flyback, the RC snubber-assisted flyback, and the proposed active clamp flyback. In the traditional flyback operating at 20 kHz, the main MOSFET experiences a high drain-source voltage (V_{DS_main}) of 380 V with severe ringing due to transformer leakage inductance and hard switching, leading to high voltage stress and reduced reliability. The RC snubber configuration, also at 20 kHz, lowers the peak V_{DS_main} to 320 V and effectively damps oscillations, though at the expense of minor energy loss across the snubber components. In contrast, the proposed active clamp converter operating at 50 kHz significantly reduces the main switch voltage stress to 140 V and introduces a controlled clamp voltage (V_{DS_clamp}) of only 25 V, both with minimal oscillation. This improvement results from soft-switching operation and energy recovery enabled by the active clamp circuit, which recycles the leakage energy rather than dissipating it as heat. Consequently, the active clamp configuration achieves the highest efficiency, reduced electromagnetic interference, and enhanced overall performance compared to the other two configurations. The experiments confirm that the proposed Active Clamp Flyback converter achieves efficient energy transfer, reduced voltage stress, and improved switching performance compared to conventional hard-switched flyback designs.

Quantitatively, the RC snubber provides a moderate stress reduction of approximately 15.8% relative to the conventional flyback case, while the active clamp converter achieves approximately 63.2% reduction in main-switch voltage stress. This comparison shows that passive damping can reduce ringing but cannot recover leakage energy, whereas the active clamp topology simultaneously suppresses voltage overshoot and supports soft-switching energy recovery. The result also strengthens the hardware relevance of the proposed method, as lower VDS stress increases the device derating margin and reduces the probability of avalanche-related failure during repetitive operation.

Table 2. Experimental results summary across the three configurations

Configuration	F_s	V_{DS_MAIN}		V_{DS_CLAMP}		Remarks
		Max	Osc	Max	Osc	
Traditional flyback	20 kHz	380 V	High	-	-	High voltage stress, severe ringing
RC snubber	20 kHz	320 V	Low	-	-	Improved damping, minor loss
Active clamp	50 kHz	140 V	Low	25 V	Low	Soft switching, energy recovery, and highest efficiency

To clarify the experimental comparison, Figure 8 summaries the normalized main-switch voltage stress for the three configurations tested. The conventional flyback converter is used as the reference value of 1.0, while the RC snubber and active clamp configurations are normalized against this value. The result shows that the active clamp topology provides the largest reduction, lowering the normalized stress to approximately 0.37 of the conventional case. In addition, the ZVS transition in Figure 7 is identified by the reduction of V_{DS_main} to a low level before the main gate signal turns on, confirming that the deadtime interval allows the resonant discharge process to occur before switch activation. However, a full simulation-versus-experiment overlay and a load-dependent efficiency curve are not included in the present experimental scope, as this study prioritizes measured switching-stress mitigation in the 100 W prototype. These additional visualization datasets will be considered in future work, along with higher-power and dynamic-load validation.

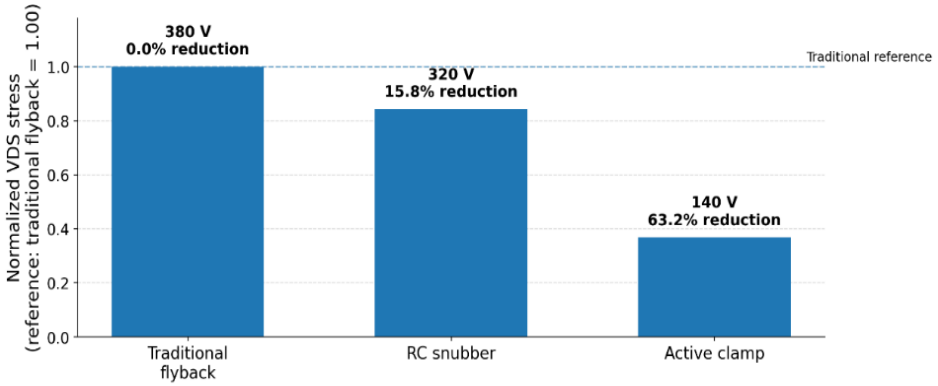

Figure 8. Normalized main-switch voltage-stress comparison based on experimental peak VDS values

The proposed active clamp flyback converter is qualitatively compared with RCD clamp, resonant reset, and quasi-resonant flyback topologies. RCD clamp circuits effectively limit voltage spikes but dissipate leakage energy, resulting in lower efficiency. Resonant and quasi-resonant approaches improve soft-switching performance but often introduce higher control complexity or variable switching frequency. In contrast, the proposed active clamp converter enables energy recovery from leakage inductance while maintaining fixed-frequency operation, achieving reduced switching stress and improved efficiency.

Although no quantitative THD, efficiency, or EMI measurements are included, literature indicates that active clamp converters generally provide better switching performance and lower EMI compared to dissipative clamp methods. This improvement is attributed to reduced voltage overshoot and controlled switching transitions. Overall, the proposed topology offers a balanced trade-off between efficiency, complexity, and performance.

4. CONCLUSION

This study investigated the performance enhancement of a flyback converter through switching device selection and active clamp circuit implementation for high-efficiency isolated DC–DC conversion. Experimental results show that the conventional flyback converter suffers from significant voltage stress due to transformer leakage inductance, with peak drain-source voltage reaching approximately 380 V. The inclusion of an RC snubber reduced the voltage stress to approximately 320 V by damping oscillations, although at the expense of dissipative energy loss. In contrast, the proposed active clamp flyback converter significantly improved performance by reducing the peak voltage stress to approximately 140 V and enabling ZVS through coordinated tuning of the resonant inductance L_r, clamp capacitance C_{clamp}, and a 550 ns deadtime interval. This confirms that proper coordination of resonant parameters is critical for achieving soft-switching operation and reducing switching losses in SiC-based converters. From an application perspective, the results demonstrate strong relevance to modern power electronics systems, particularly in solar photovoltaic microinverters, electric vehicle (EV) auxiliary power supplies, battery energy storage systems, and microgrid interface converters. These systems require compact, high-efficiency, and electrically isolated DC–DC converters capable of operating reliably under high-frequency switching and dynamic load conditions. In addition, the findings highlight that active clamp energy recovery effectively transforms leakage inductance from a source of loss and stress into a controllable resonant mechanism that improves efficiency, reliability, and thermal performance. This strengthens the practical viability of SiC-based active clamp flyback converters for next-generation renewable energy and electrified transportation applications. Finally, future work will extend this study to higher power levels, detailed efficiency mapping, EMI spectral analysis, and long-term thermal cycling validation to further confirm scalability and robustness under real operating conditions.

FUNDING INFORMATION

This research is funded by Institut Teknologi Padang under grant number 83/27.O10.1.2/PN/VIII/2025.

AUTHOR CONTRIBUTIONS STATEMENT

This journal uses the Contributor Roles Taxonomy (CRediT) to recognize individual author contributions, reduce authorship disputes, and facilitate collaboration.

Name of Author	C	M	So	Va	Fo	I	R	D	O	E	Vi	Su	P	Fu
Fauzan Ismail	✓	✓	✓	✓	✓	✓	✓	✓	✓	✓			✓	
Taufal Hidayat		✓		✓	✓	✓		✓		✓			✓	✓
Maaspaliza Azri		✓		✓	✓			✓		✓	✓			
Yushaizad Yusof				✓	✓					✓				

C : **C**onceptualization
M : **M**ethodology
So : **So**ftware
Va : **Va**lidation
Fo : **Fo**rmal analysis
I : **I**nvestigation
R : **R**esources
D : **D**ata Curation
O : Writing - **O**riginal Draft
E : Writing - Review & **E**diting
Vi : **Vi**sualization
Su : **Su**pervision
P : **P**roject administration
Fu : **Fu**nding acquisition

CONFLICT OF INTEREST STATEMENT

The authors state no conflict of interest.

DATA AVAILABILITY

The data that support the findings of this study are available on request from the corresponding author, [FI]. The data, which contain information that could compromise the privacy of research participants, are not publicly available due to certain restrictions.

REFERENCES

[1] D. Ferreira *et al*., "Isolated quasi-switched boost integrated t-type DC-DC converter for DC microgrid," in *2024 13th International Conference on Renewable Energy Research and Applications (ICRERA)*, IEEE, Nov. 2024, pp. 321–326, doi: 10.1109/ICRERA62673.2024.10815253.

[2] G. Tian, S. Chen, X. Ding, J. Peng, and Z. Kou, "Isolated high step-up soft-switching quasi-Z-source DC–DC converter," *IEEE Access*, vol. 12, pp. 49927–49936, 2024, doi: 10.1109/ACCESS.2024.3381198.

[3] K. R. Kothapalli, M. R. Ramteke, and H. M. Suryawanshi, "ZVS–ZCS high step-up/step-down isolated bidirectional DC–DC converter for DC microgrid," *IEEE Transactions on Power Electronics*, vol. 38, no. 6, pp. 7733–7745, Jun. 2023, doi: 10.1109/TPEL.2022.3208455.

[4] R. S. Widagdo, P. Slamet, A. H. Andriawan, R. Hartayu, Santoso, and B. Hariadi, "Design of zero current switching flyback converter for power efficiency in solar power system," in *2024 International Conference on Electrical Engineering and Computer Science (ICECOS)*, IEEE, Sep. 2024, pp. 71–76, doi: 10.1109/ICECOS63900.2024.10791204.

[5] D. E. Giraldo-Hernández *et al.*, "Large-signal nonlinear average model for a voltage-controlled flyback converter," *Energies*, vol. 18, no. 3, Jan. 2025, doi: 10.3390/en18030451.

[6] M. Abbasi *et al.*, "A new dual-purpose flyback-based DC–DC/AC converter with dynamic voltage gain," in *2024 IEEE Applied Power Electronics Conference and Exposition (APEC)*, IEEE, Feb. 2024, pp. 366–369, doi: 10.1109/APEC48139.2024.10509212.

[7] S. Qazi, L. de Oliveira Baumann, K.-B. Park, F. Canales, and T. B. Soeiro, "A hybrid si-sic flyback converter for auxiliary power supplies in DC ship grids," in *2024 IEEE Applied Power Electronics Conference and Exposition (APEC)*, IEEE, Feb. 2024, pp. 3157–3162, doi: 10.1109/APEC48139.2024.10509323.

[8] J.-S. Yoo, J.-O. Baek, and T.-Y. Ahn, "A high-efficiency qr flyback DC–DC converter with reduced switch voltage stress realized by applying a self-driven active snubber (SDAS)," *Energies*, vol. 16, no. 3, Jan. 2023, doi: 10.3390/en16031068.

[9] W. Haider and Q. P. Ha, "A lossless passive snubber for soft-switching of flyback converters," in *2024 IEEE 19th Conference on Industrial Electronics and Applications (ICIEA)*, IEEE, Aug. 2024, pp. 1–6, doi: 10.1109/ICIEA61579.2024.10664895.

[10] X. Guo, S. Wu, Y. Zhang, C. Dou, and Y. Chi, "Optimal design of high frequency transformer for high power density flyback converter," *IEEE Transactions on Circuits and Systems II: Express Briefs*, vol. 69, no. 11, pp. 4399–4403, Nov. 2022, doi: 10.1109/TCSII.2022.3184724.

[11] L. Zheng, R. P. Kandula, K. Kandasamy, and D. Divan, "New modulation and impact of transformer leakage inductance on current-source solid-state transformer," *IEEE Transactions on Power Electronics*, vol. 37, no. 1, pp. 562–576, Jan. 2022, doi: 10.1109/TPEL.2021.3101811.

[12] J.-H. Choi, H.-M. Kwon, and J.-Y. Lee, "Design of a 3.3 kw/100 khz EV charger based on flyback converter with active snubber," *IEEE Transactions on Vehicular Technology*, vol. 71, no. 7, pp. 7161–7170, Jul. 2022, doi: 10.1109/TVT.2022.3168625.

[13] B. A. Kumar and M. Alam, "Evaluating wide band gap semiconductor hybrid switches: a comparative analysis," in *2024 IEEE International Students' Conference on Electrical, Electronics and Computer Science (SCEECS)*, IEEE, Feb. 2024, pp. 1–6, doi: 10.1109/SCEECS61402.2024.10482225.

[14] T. Van Do, J. P. F. Trovao, K. Li, and L. Boulon, "Wide-bandgap power semiconductors for electric vehicle systems: challenges and trends," *IEEE Vehicular Technology Magazine*, vol. 16, no. 4, pp. 89–98, Dec. 2021, doi: 10.1109/MVT.2021.3112943.

[15] J. Cruz-Cozar, A. Medina-Garcia, D. P. Morales, and N. Rodriguez, "Resonant hybrid flyback: a novel topology with wide voltage range for DC microgrid applications," *Energy Reports*, vol. 9, pp. 3222–3234, 2023, doi: 10.1016/j.egyr.2023.02.027.

[16] A. Nasiri, M. R. Banaei, S. M. Alavi, and S. Hosseinzadeh, "A new control method for magnetron lamp power supply using forward-flyback converter with active clamp," *IEEE Transactions on Plasma Science*, vol. 51, no. 10, pp. 3080–3086, 2023, doi: 10.1109/TPS.2023.3311317.

[17] P. C. Tseng, K. I. Hwu, Y. L. Chen, and J. J. Shieh, "Active-clamp dual-transformer ZVS flyback converter," *Energies*, vol. 18, no. 13, 2025, doi: 10.3390/en18133331.

[18] L. Deng, G. Zhou, Y. Li, and H. Yu, "GaN-based active clamp flyback converter realizing soft-switching over wide voltage range through auxiliary leakage inductor," in *PEDG 2023 - 2023 IEEE 14th International Symposium on Power Electronics for Distributed Generation Systems*, 2023, pp. 202–207, doi: 10.1109/PEDG56097.2023.10215286.

[19] H. Li, S. Li, W. Xiao, and S. Y. R. Hui, "A modulation method for capacitance reduction in active-clamp flyback-based AC-DC adapters," *IEEE Transactions on Power Electronics*, vol. 37, no. 8, pp. 9455–9467, 2022, doi: 10.1109/TPEL.2022.3157743.

[20] R. K. Kokkonda, R. Beddingfield, S. Bhattacharya, B. Carsten, and B. Varga, "A novel transformer leakage energy recovery active clamp control technique for high power AC/DC flyback converters," in *2023 IEEE Applied Power Electronics Conference and Exposition (APEC)*, IEEE, Mar. 2023, pp. 1238–1245, doi: 10.1109/APEC43580.2023.10131320.

[21] T. Nouri, "Performance improvement of a zero-voltage switching interleaved high step-up DC DC.pdf," *IET Power Electronics*, vol. 16, pp. 1913–1928, 2023.

[22] T. N. T. Tran, H. Y. Xu, and J. M. Wang, "Development of active-clamp flyback converter for improving light-load efficiency," *IEEE Journal of Emerging and Selected Topics in Power Electronics*, vol. 12, no. 3, pp. 2456–2469, 2024, doi: 10.1109/JESTPE.2024.3387549.

[23] D.-H. Kown and J.-K. Kim, "Active clamp forward converter with a new switch control technique for reducing transient voltage overshoot," in *2023 11th International Conference on Power Electronics and ECCE Asia (ICPE 2023 - ECCE Asia)*, IEEE, May 2023, pp. 1738–1744, doi: 10.23919/ICPE2023-ECCEAsia54778.2023.10213953.

[24] A. B. Mirza, Y. Xie, S. S. Vala, and F. Luo, "Impact of pcb parasitic capacitance on switching transients in split-phase inverter utilizing to-247 sic devices," *2023 IEEE Energy Conversion Congress and Exposition, ECCE 2023*, pp. 5504–5509, 2023, doi: 10.1109/ECCE53617.2023.10362372.

[25] M. Cai, O. Wasynczuk, and M. Saeedifard, "A voltage-edge-rate-limiting soft-switching inverter for wide-bandgap devices," *2018 IEEE 6th Workshop on Wide Bandgap Power Devices and Applications, WiPDA 2018*, pp. 271–278, 2018, doi: 10.1109/WiPDA.2018.8569093.

[26] A. Medina-Garcia, J. Cruz-Cozar, D. P. Morales-Santos, N. Rodriguez, and M. Schlenk, "A high-efficiency isolated wide voltage range DC-DC converter using wbg devices," *IEEE Access*, vol. 10, pp. 84818–84825, 2022, doi: 10.1109/ACCESS.2022.3197644.
[27] T. Xia *et al.*, "A hybrid three-level hybrid switch (hybrid 2) active neutral-point-clamped converter with optimal switching strategy," *IEEE Journal of Emerging and Selected Topics in Power Electronics*, vol. 13, no. 3, pp. 3046–3058, Jun. 2025, doi: 10.1109/JESTPE.2024.3525359.

BIOGRAPHIES OF AUTHORS



Fauzan Ismail received his Bachelor of Engineering (B.E.) degree from the University of Andalas, Padang, Indonesia, in 2004, and his Master of Engineering Science (M.Eng.Sc.) degree and Ph.D. in power electronics from the University of Malaya, Kuala Lumpur, Malaysia, in 2011 and 2024, respectively. He is currently a postdoctoral researcher at the University of Malaya Power Energy Dedicated Advanced Centre (UMPEDAC), University of Malaya. He joined the Department of Electrical Engineering at Padang Institute of Technology as a lecturer in 2016. His research interests include power electronics and renewable energy. He can be contacted at email: fauzanismail@itp.ac.id.



Taufal Hidayat received his Bachelor of Engineering (B.Eng.) and Master of Engineering (M.Eng.) degrees in electrical engineering from the University of Indonesia, Indonesia, in 2012 and 2013, respectively. He received his Ph.D. from the Department of Electrical and Computer Engineering at King Abdulaziz University (KAU), Saudi Arabia. He is currently a lecturer in the Department of Electrical Engineering at Institut Teknologi Padang, West Sumatra, Indonesia. His research interests include renewable and alternative energy, wind farm layout optimization, and metaheuristic algorithms. He can be contacted at email: taufal.hidayat@itp.ac.id.

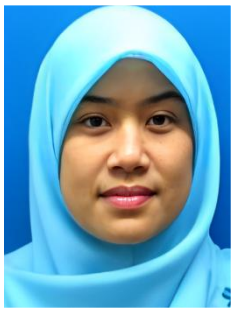

Maaspaliza Azri was born in Malacca, Malaysia, in 1977. She received her Bachelor of Engineering (Honours) degree in Electrical Engineering from Universiti Teknologi MARA, Shah Alam, Malaysia, in 2001, and her Master of Science (M.Sc.) degree in Electrical Power Engineering from Universiti Putra Malaysia, Serdang, Malaysia, in 2004. She received her Ph.D. from the UM Power Energy Dedicated Advanced Centre (UMPEDAC), University of Malaya, Kuala Lumpur, Malaysia, in 2014. Since 2015, she has been a senior lecturer at the Faculty of Electrical Technology and Engineering, Universiti Teknikal Malaysia Melaka (UTeM). From 2018 to 2020, she served as Head of the Department of Electrical Engineering at the Faculty of Electrical Engineering, UTeM. She is a Chartered Engineer registered with the Institution of Engineering and Technology (IET), UK, and has been a Professional Engineer registered with the Board of Engineers Malaysia (BEM) since 2023. Her research interests include power electronics and renewable energy. She can be contacted at email: maaspaliza@utem.edu.my.



Yushaizad Yusof received his Bachelor of Engineering (B.Eng.) degree from Kagoshima University, Japan, in 1999, his Master of Engineering (M.Eng.) degree from Universiti Teknologi Malaysia (UTM) in 2002, and his Ph.D. from Universiti Malaya (UM) in 2019. He is currently affiliated with the Faculty of Engineering and Built Environment (FKAB) at Universiti Kebangsaan Malaysia (UKM). His research interests include power electronics and motor drives. He can be contacted at email: yushaizad@ukm.edu.my.